The interplay between molecular structure and dielectric properties in ionic liquids: A comparative study

Boumediene Haddad, Achraf Kachroudi, Gamal Turky, El Habib Belarbi, Abdelkader Lamouri, Didier Villemin, Mustapha Rahmouni, Alain Sylvestre, El Habib Belarbi

The interplay between molecular structure and dielectric propertiesin ionic liquids: A comparative study

Boumediene Haddad [a,b,c], Achraf Kachroudi [d], Gamal Turky [e], El Habib Belarbi [b,*], Abdelkader Lamouri [a], Didier Villemin [c], Mustapha Rahmouni [b], Alain Sylvestre [d]

[a] Chemistry Laboratory of Synthesis, Properties, and Applications (CLSPA-Saida), University of Saida, Algeria
[b] Synthesis and Catalysis Laboratory LSCT, University of Tiaret, Tiaret, Algeria
[c] LCMT, ENSICAEN, UMR 6507 CNRS, University of Caen, 6 bd Ml Juin, 14,050 Caen, France
[d] Univ. Grenoble Alpes, G2Elab, F-38000 Grenoble, France
[e] Department of Microwave Physics and Dielectrics, National Research Centre, 33 El-Bohouth St., (Former El-Tahrir St.), Dokki, Giza, P.O. 12622, Egypt.

Keywords:
Ionic liquids
Protonated
C-2 methylation
Thermal properties
Dielectric spectroscopy
Relaxation phenomena

In this work, C2-Methylated [C_3DMIM^+][I^-] versus C2-Protonated [C_3MIM^+][I^-] Imidazolium-Based Ionic Liquids containing iodide anion, have been synthesized and characterized using ^1H and ^{13}C NMR spectroscopy methods. In order to investigate the methylation effect on thermal properties, we rely to three additional thermal analysis techniques. The thermal behavior confirmed that the methylated [C_3DMIM^+][I^-] IL is more stable than the protonated one [C_3MIM^+][I^-].The conductivity and dielectric relaxation properties of both ILs have been investigated in the frequency range [10^{-2}, 10^7 Hz] and the temperature ranging between −30 °C and 60 °C. Dielectric permittivity studies show that the substitution of the hydrogen atom by a methyl group has a significant impact in both the realε' and imaginary ε'' parts. In addition, the analysis of the observed relaxation times for the protonated IL [C_3MIM^+][I^-] showed Arrhenius-type temperature dependence for the temperatures ranging between 20 °C and 60 °C $^-$ and VFT temperature dependence for the temperatures ranging between −20 °C and 20 °C$^-$, while, the methylated IL [C_3DMIM^+][I^-] showed Vogel-Fulcher-Tamman-type temperature dependence in the entire investigated temperature range − 30 °C to 60 °C. The representation of σ'' (ν, T) shows the buildup of the electrochemical double layer and interfacial effect. However the real part of complex conductivity follows the empirical Jonscher equation. The determined dc-conductivity of both investigated Ionic liquids present a new behavior regarding the thermal activation an anomalous thermal activation behavior. It follows an Arrhenius relation at lower temperatures and then reach a steady state values at higher temperatures.

1. Introduction

Recently, ionic liquids (ILs) become of great interest for researchers and industrialistsdue totheir interesting and unique physicochemical properties. These include the following properties: very low vapor pressure [1],liquid at room temperature [2], non-flammability [3], high solubility power [4], good solvent capacity [5] potential products as designer solvents for catalytic and chemical applications as well asin processes relating to transport and storage of energy [6]. For this reason, they have been deeply investigated and explored as novel electrolytes for electrochemical devices including rechargeable lithium batteries and hybrid super capacitors [7].the reliability study of an ionic liquid for its use as electrolyte, requires its molecular structure analysis as function of its physicochemical and electrical properties [8–10].So, establishing this relationships analysis will be the key parameter for understanding the how to optimise the accumulation of charge carriers at the metal electrode/ ionic liquids' interface. From electrochemical point of view, the thermal stability, low melting point, dielectric constant, electrochemical window, and electrical conductivity are important parameters that determine the suitability of an IL for the desired application [11]. In this context, many studies were reported in the literature investigating the thermal [12–15], dielectric and conductive properties of ionic liquids [16–20]. The aim of these works was to identify, investigate and understand the dynamic behavior and ionic transport in these fluids. During last year's, several experimental and simulation studies have indicated that exchanging the proton at C2 position in the cation of imidazolium-based ILs by a methyl group has an important impact in their physicochemical properties. Tremendous effects on the melting point, the viscosity, the vaporization enthalpy, the density and the conductivity were reported [21–25].Weingärtner [26] showed that the impact of potential hydrogen bonds at C(2)-H of the 1-alkyl-3-methylimidazolium cationon the static dielectric constant is not quite clear as the influence was rather small. This was confirmed by Huang

* Corresponding author.
E-mail address: belarbi@univ-tiaret.dz (E.H. Belarbi).

et al. [27], who also found that the substitution of the acidic hydrogen at C2 by a methyl group does not notably affect the static permittivity, ε_s. Endo et al. [28] studied the effect of C2 methylation on the rotational dynamics of alkyl imidazolium bromide based ILs by estimating the rotational correlation time obtained from the experimentally measured τ_1-relaxation time. Their results show that an unusually small increase in the rotational correlation time at the root of the butyl chain has been observed upon the C2 substitution in a comparison between [BMMIM][Br] and [BMIM][Br].

Several works concerning chemical and physical properties highlighted the differences between the C2-methylated ILs and their C2-protonated analogues. However, according to the authors' knowledge, there are no reported works in the literature dealingwith the effect of methylation on the dielectric properties.

In the present paper, we report the effect of C2 methylationon the thermal and dielectric properties of two glass forming imidazolium ionic liquids (ILs).The compounds 1-methyl-3-propylimidazolium [C_3MIM^+][I^-] and 1,2-dimethyl-3-propylimidazolium [C_3DMIM^+][I^-] were synthesized and theirchemical structures were confirmed by ^1H, ^{13}C-NMRspectroscopy. The thermal properties were investigated in the temperature range [25 °C, 350 °C] using thermogravimetric analysis (TGA), differential thermal analysis (DTA), and differential scanning calorimetry (DSC)from −100 to 100 °C. Dielectric measurements were performed in the frequency range [10^{-1},10^7Hz] and temperature ranging between −30 °C to 60 °C allowing us to probethe different relaxationmechanisms and the associated activation energies. The variation of dielectric and electrical parameters allows us to analyzethe effect of C2 methylation on the relaxation dynamics and the charge-carrier mobility.

2. Experimental

The chemical reagents used in this study are: 1-methylimidazole (>99%), 1,2-dimethylimidazole (98%), and propyl iodide (98%). They were purchased from Fluka and used as received. Deionized H_2O was obtained with a Millipore ion-exchange resin deionizer. ^1H NMR (400 MHz), ^{13}C NMR (100.6 MHz), spectra were recorded on a DRX 400 MHz spectrometer. The chemical shifts (δ) are given in ppm and referenced to the internal solvent signal namely TMS and $CFCl_3$, respectively.

2.1. General procedure for the synthesis of investigated ILs

The synthetic routes used to prepare both [C_3MIM^+][I^-] and [C_3DMIM^+][I^-] are reported in our previous work [29]. Briefly, [C_3MIM^+][I^-] and [C_3DMIM^+][I^-]were prepared in high yields; (87%) from 1-methylimidazole and (92%) for 1,2-dimethylimidazole precursors and propyl iodide. The chemical structures of the target ILs are shown in Fig. 1. Prior to use, both ionic liquids were dried under vacuum at 70 °C overnight, and kept either under nitrogen or in a vacuum desiccator to protect them from ambient moisture. Moreover,inorder to further improve the purity, the obtained ILs were dried on a high-vacuum line ($P < 10^{-5}$ bar) for 4 days at approximately a temperature of 40 °C.To confirm the structures of both ILs and the absence of residuals from the synthesis, the obtained ILs were confirmed using ^1H,^{13}C asreported inour previous work [29].The water content in [C_3MIM^+][I^-] and [C_3DMIM^+][I^-] was below 350 ppm. This measure was carried out by colometricKarl Fischer titration, performed by a Metrohm 831 [29].

2.2. TGA and DTA measurements

TGA and DTA measurements were performed using a Setaram Setsys 1200 instrument, under an inert helium flux of 60 ml/min, heating from 25 °C with a rate of 5 °C/min.

2.3. DSC measurements

Differential scanning calorimetrywascarried out using a *TA Q20* instrument applying a rate of 5 °C/min between −100 and 100 °Cto identify the phase transition temperatures.

2.4. Dielectric spectroscopy

Dielectric measurements were performed in the temperature range [−30 °C,60 °C] and in the frequency range between 10^{-1} and 10^7 Hz using a Novocontrol Alpha impedance analyzer. All the measurements are carried out isothermally, where the temperature was controlled by a QuatroNovocontrolcryo-system with a stability of 0.1 K. The output data are the dielectric permittivity $\boldsymbol{\varepsilon^*}$ and the complex conductivity σ^*. The relationship between both parameters is expressed as:

$$\sigma^*(\boldsymbol{\omega}, \boldsymbol{T}) = \boldsymbol{i\varepsilon_0\omega\varepsilon} * (\boldsymbol{\omega}, \boldsymbol{T}) \quad (1)$$

implying that $\sigma' = \varepsilon_o\omega\varepsilon''$and $\sigma'' = \varepsilon_o\omega\varepsilon'$,where $\varepsilon_o$is the free-space permittivity ,ω is the radial frequency = 2πf (f is the frequency), ε' and ε'' are the real and imaginary parts of the dielectric permittivity, respectively. For more details see Refs. [30–33].

3. Results and discussion

3.1. Thermal properties

The knowledge of the thermal properties of ILs, such as the glass transition, melting and decomposition temperature is crucial from an

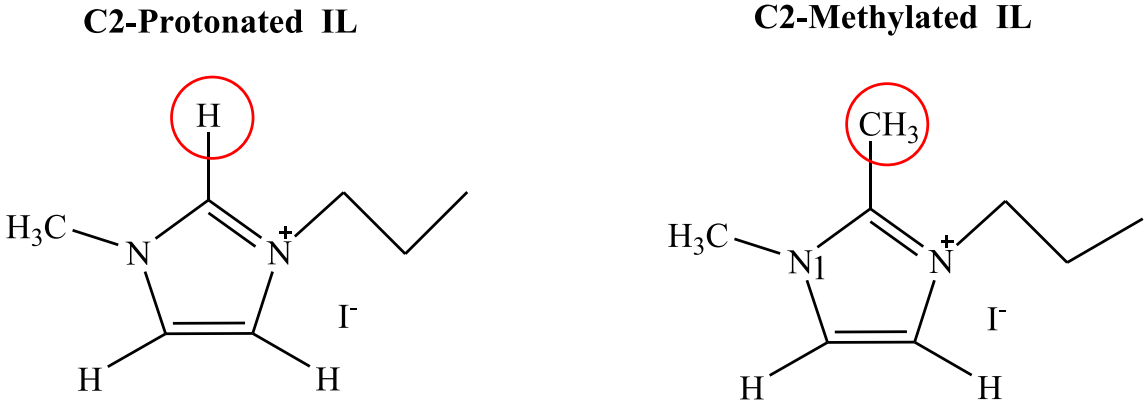

Fig. 1. Structures of [C_3MIM^+][I^-]and [C_3DMIM^+][I^-].

engineering point of view as they are important parameters for determining process conditions and also to identify the impact and contribution of each transition on the dielectric and electric phenomena.In this context, threecomplementary thermal analysis techniqueswere used: TGA, DTG and DSC. The obtained results with TGA and DTG are presented in Figs. 2 and 3. The values corresponding to the maximum decomposition temperature, which was found from derivative peaks, are reported in Table 1.

Comparing the thermal stability of both ILs, the methylated [C_3DMIM^+][I^-] IL is more stable than the protonated one[C_3MIM^+][I^-]. In fact, the C(2) methylation increased the decomposition temperature from 308 to 324 °C. Ngo et al. [34], Awad et al. [35], and Maton et al. [36] reported similar observations. The thermal decomposition of both ILs occurs in the temperature range [300 °C, 400 °C], which reaches 100% at 342 °C for [C_3MIM^+][I^-] and at 362 °C for the methylated IL.

From the DSC curve, the protonated IL [C_3MIM^+][I^-] does not show a glass transition during the heating scan, while in the methylated case a small peak at −25 °C can be observed as result of a deviation from the thermo-grams baseline under the same experimental conditions used corresponding to the glass transition temperature. Additionally, a clear exothermic peak at 29 °C was observed in this latter IL. This exothermic peak probably reflects the melting process.

3.2. Dielectric analysis

The real part and the imaginary part of complex dielectric permittivity and conductivity as function of temperature and frequency for the C2-protonated [C_3MIM^+][I^-] and C2-methylated [C_3DMIM^+][I^-] are presented in Figs. 4 and 5 respectively.

It is found that the real part of the permittivity Figs. 4(a) and 5 (a) decreases with the increase of frequency. The appearance of this process is more clearly seen in ε''vs frequency plot (Figs. 4(b) and 5 (b)). A relaxation process is detected through the presence of a strong dispersion in $\varepsilon'(\omega)$, the high value of permittivity at low frequencies is attributed to the electrode polarization phenomenon occurring as a result of an accumulation of ions near the electrodes [37–39]. Comparing the variations of ε' and $\varepsilon''$for both ILs, the temperature dependence of the dielectric permittivity exhibits distinct differences. These differences are expected due to the substitution of the hydrogen atom by a methyl group with its own properties. It can be concluded that the substitution contributes to the increase of both the real (ε') and imaginary (ε'') parts of the dielectric permittivity of the C2-methylated IL .This phenomenon could be attributed to the hindrance effect of the –CH_3 group [40,41]. In addition, it could come from the absence of the relaxation pathway above the C2 atom. This might be responsible for the slower ion transport of the methylated ionic liquids as was previously reported in the literature [42]. Another important insight is that the methylation at the C2 position leads to a reduction of the free movement of the anion around the cation as the number of potential bonding sights at the imidazolium ring is reduced.

The relaxation mechanisms can also be observed via the dielectric loss tangent *tanδ* defined as:

$$\boldsymbol{tan\delta(f)} = \frac{\boldsymbol{\varepsilon''}}{\boldsymbol{\varepsilon'}} \tag{2}$$

The relaxation time is obtained by studying tanδ as a function of frequency and temperature. of the variations of *tanδ* at different frequencies and temperatures of [C_3MIM^+][I^-] and [C_3DMIM^+][I^-] are presented in Fig. 6.

The dielectric loss peak maxima allow us to determine the relaxation time τ.

It seems that both ILs become flexible and show relaxation peaks in the frequency range between 10^2 and 10^6 Hz. As clear observed in Fig. 6 (a), the relative peak intensity for the C2-Protonated [C_3MIM^+][I^-] is increasing with increasing temperature up to a temperature of 20 °C, indicating that the relaxation is thermally activated. It can be easily observed that the detected loss tangent peaks in the case of the protonated ionic liquid [C_3MIM^+][I^-] has a more pronounced amplitude compared to those detected in the case of the methylated [C_3DMIM^+][I^-] (Fig. 6(b)). This suggests that the the methyl group in the C2-position inhibits the diffusion of ions [40,42,44,45] and enforces a restricted rotation of the propyl chain, promoting alkyl chain association between cations and thus contributing to a decrease of the relaxation mechanisms.

In order to study more deeply the mechanisms involved in the relaxation and especially those related to the thermal activation, the loss peak frequency $f_{max}$was analyzed as a function of 1000/*T*. The resulting Arrhenius plot is presented in Fig. 6. The studied ILs show two different behaviors:

a) Arrhenius-type temperature dependence in the temperature range of 20–60 °C for the protonated IL [C_3MIM^+][I^-].
b) VFT-like temperature dependence in the temperature range of −20–20 °C for the protonated IL [C_3MIM^+][I^-] and in the entire investigated temperature range — 30 °C to 60 °C for the methylated IL [C_3DMIM^+][I^-].

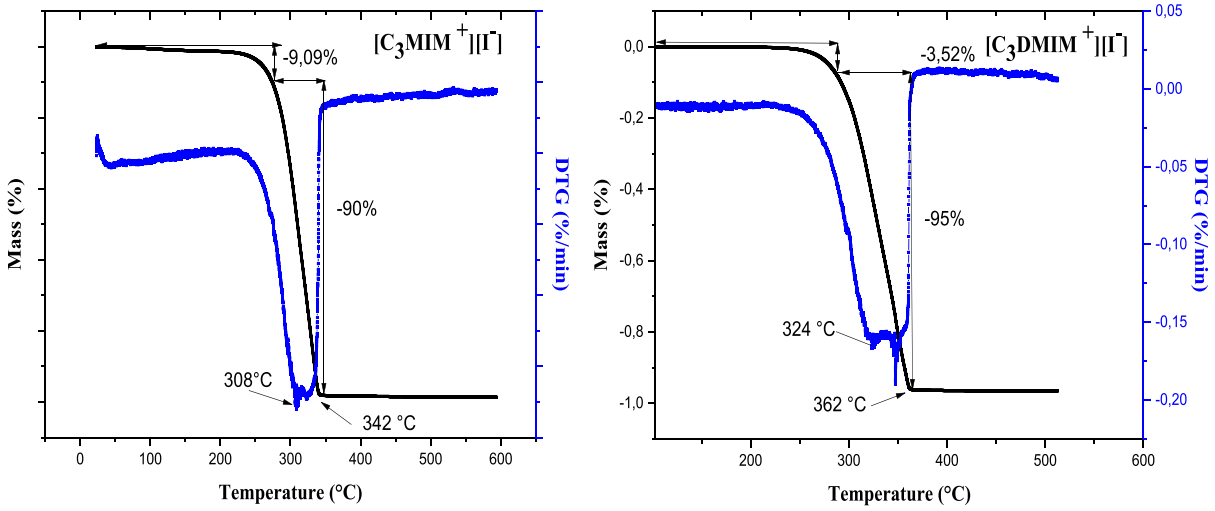

Fig. 2. TGA and DTG curves of C2-Methylated [C_3DMIM^+][I^-]versus C2-Protonated [C_3MIM^+][I^-] Imidazolium-Based Ionic Liquids.

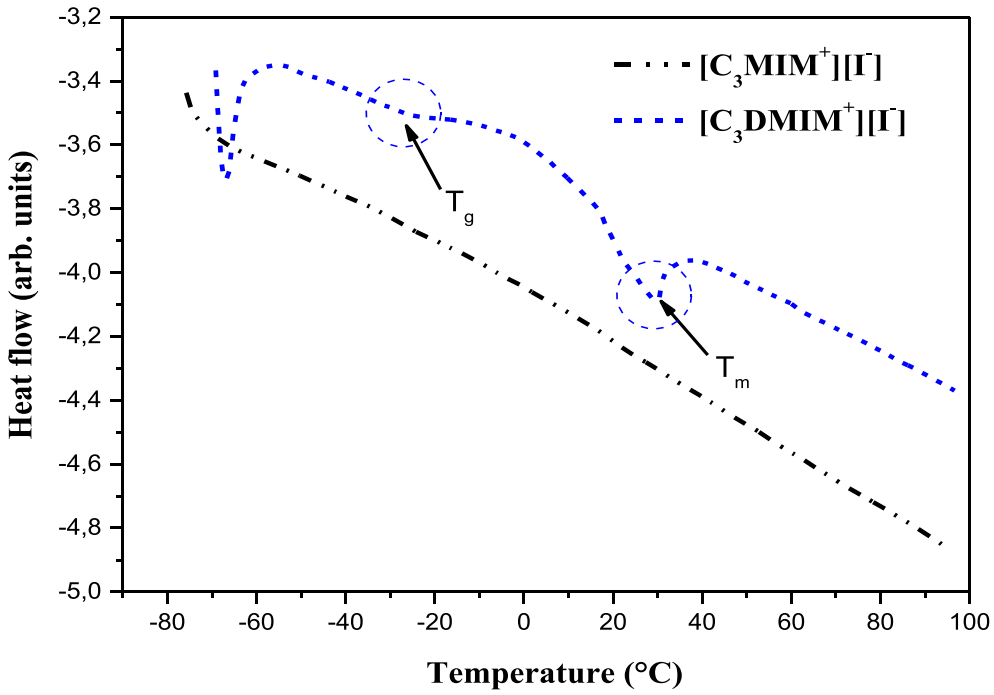

Fig. 3. DSC curves of C2-Methylated [C_3DMIM^+][I^-] versus C2-Protonated [C_3MIM^+][I^-] Imidazolium-Based Ionic Liquids.

The obtained results are comparable to those previously obtained for polymerized ionic liquids as reported by Nakamura et al. [46]. The observed behavior changing from VFT to Arrhenius is attributed to the petitive ion-pair formation and dissociation processes, and counterion diffusion associated with the motion of cation groups [47]. The blue and redlines in Fig. 7 presents the best mean square fit curves for both ILs using the VFT and Arrhenius laws, respectively, given by the following equations:

$$\tau = \tau_{OA} \exp\left[-\frac{E_1}{k_b T}\right] \quad (3)$$

$$\tau = \tau_{OVFT} \exp\left[-\frac{E_2}{k_b (T - T_0)}\right] \quad (4)$$

Subscribes A and VFT are used to distinguish between the Arrhenius and VFT laws, respectively. E_1 and E_2 are the activation energies, T_0 is the Vogel temperature, τ_{OA}, τ_{OVFT}, and $k_b$are the pre-exponential factors and the Boltzmann constant, respectively. Activation energies are extracted from the best fits reached in Fig. 6 and are reported in Table 2.

According to the values reported in Table 2 using the VFT equation, the [C_3MIM^+][I^-] IL activation energy is significantly higher compared to the [C_3DMIM^+][I^-] IL activation energy (about six times higher in the case of C2-Protonated IL). This result makes sense, as the activation energy of the relaxation mechanisms are related to the cooperative motion and the conformation changes in both ILs. In addition, this mechanism is related to the rotation of the propyl group and it is coupled with the structural relaxation [43]. Consequently, the activation energy indicates a local re-arrangement.

Table 1
Comparison of thermal properties of C2-methylated versus c2-protonated imidazolium-based ionic liquids.

ILs	P_s (25 °C)[a]	T_g(°C)[b]	T_m(°C)[c]	$T_{d\ (TGA)}$(°C)[d]	$T_{Td(TGA)}$(°C)[e]
[C_3MIM^+][I^-]	Liquid	–	–	308	342
[C_3DMIM^+][I^-]	Solid	−25	29	324	362

– =Not detected.
[a] Ps Physical state at 25 °C.
[b] Glass transition temperature (T_g).
[c] Melting point (from DSC onset of the endothermic peak) (T_m).
[d] Decomposition temperature (from TGA onset decomposition peak) ($T_{d(TGA)}$).
[e] Total Decomposition temperature (from TGA decomposition peak) ($T_{Td(TGA)}$).

3.3. Conduction mechanisms

The AC-conductivities of both ILs are presented as function of frequency for different temperatures in Figs. 4(c) and 5(c). The conductivity is found to increases with frequency. Moreover, at high frequencies, the conductivity values rapidly increase in the entire temperature range. In contrast, the values of σ' decrease with increasing temperature. As the conductivity is related to the mobility of the charge carriers, this can be explained by the higher thermal activation. Considering the conductivity at the same temperature and frequency reveals that the protonated [C_3MIM^+][I^-] IL is more conductive than the methylated [C3DMIM$^+$][I^-] one. Based on the results that were reported by Izgorodina et al. [42], the high conductivity observed in the case of the protonated ionic liquid can be explained by the stronger coordinating anion (iodide) that tends to form much shorter contacts with the imidazolium-type cation in the IL protonated case.

At the same temperature and frequency, the C2 methylated ionic liquid [C_3DMIM^+][I^-], exhibits lower values compared to [C_3MIM^+][I^-]. This is in good agreement with the commonly high viscosity and slow dynamics observed for C2 methylated ILs from experimental and computational results. Izgorodina et al. [42] found the conductivity of [C_3MIM^+][I^-] is ($\sigma = 12.6$ mS cm^{-1}) to be about six times higher than that of [C_3DMIM^+][I^-] ($\sigma = 1.95$ mS cm^{-1}) at $T = 85$ °C.

While, this latter has ($\eta = 195$ cP) to be about five times higher than that of C2-Protonated IL ($\eta = 35$ cP) at $T = 25$ °C. Also, Liao et al. [48] reported that the introduction of functional groups atthe C-2 position generally increased the viscosity and lowered the conductivity, as the conductivity of ILs largely depends on their viscosity values. Increasing the length of the alkyl side chain increases slightly the impact of the

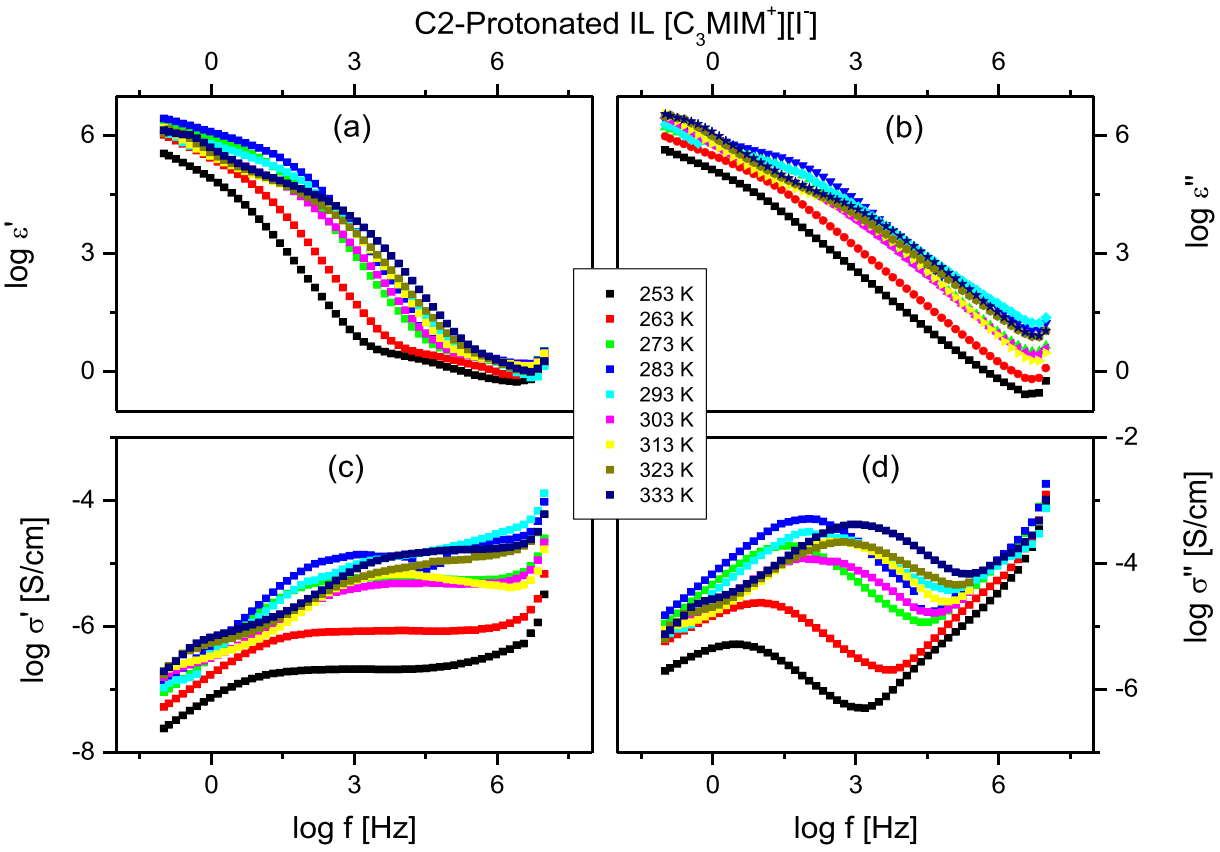

Fig. 4. Complex dielectric permittivity and conductivity as function of frequency at different temperatures for C2-Protonated [C_3MIM^+][I^-].

methylation on the conductivity difference between the protonated and C-2 methylated ionic liquids.

The electrochemical double layer formed at the interface by ions attracted towards the metal electrodes is now of great interest. Figs. 4 (d) and 5(d) show the frequency dependence of the imaginary part of the complex conductivity,σ″, at different temperatures for the sample C2- methylated [C_3DMIM^+][I^-]. The Eq. (1) given in the experimental part was used to calculate σ″ [30].

The figure shows a characteristic frequency (ν_{min}) that represents the boundary or the sharp limit of the characteristic bulk from above. Starting from this characteristic frequency, σ″ increases gradually, accompanied by increase of the real part of permittivity, ε', with decreasing frequency indicating the build-up of the electrode polarization. The values of σ″ reach a peak at another characteristic frequency, ν_{max}, at which the build-up of electrode polarization is completed. This became a main feature in ionic liquids and many other conducting polymers and glasses. Both characteristic frequencies are shifted towards higher frequencies with increasing temperatures till about 20–30 °C and then the rate of change is attenuated and the order is changed. Similar behavior was also noticed in the σ' representation (Figs. 4(c) and 5(c)).

Fig. 8 shows the frequency dependence of the real part of the complex conductivity function, σ', at three selected temperature (as representative examples) for [C_3DMIM^+][I^-]. The figure shows three regions of conductivity, with electrode polarization occurring at low frequencies, frequency independent (dc) conductivity at intermediate frequencies, and the onset of ac conductivity at higher frequencies.

Our attempt to explain the conduction mechanism by Dyre's function was not successful because of the rather large margin of error in the fitting. We have approximated the frequency dependence of σ' by the empirical Jonscher power law even it is not based on a physical model [30]:

$$\sigma'(\nu) = \sigma_{DC}\left[1 + \left(\frac{f}{f_c}\right)^n\right] \quad (5)$$

The characteristic frequency, f_c ($= 1/2\pi\tau_\sigma$) characterizes the onset of the dispersion and is related to the DC-conductivity by the empirical Barton-Nakajima-Namikawa relation (BNN): σ_{DC}~f_c. [49–51].The exponent n takes values between 0.5 and 1.By fitting using Jonscher equation (Eq. 5) to the data, both DC-conductivity values was estimated and presented against temperature for both ionic liquids under investigations as shown in Fig. 9. Like many other kinds of glass forming materials, both ionic liquids under investigations follow mostly the Arrhenius law:

$$\sigma_{dc} = \sigma_\infty \exp\left(\frac{-E_a}{K_B T}\right) \quad (6)$$

where K_B is Boltzmann constant and $\sigma_\infty$is a pre-exponential factor, at relatively lower temperatures till 10 °C for C2- methylated [C3DMIM$^+$][I^-] and 20 °C for C2-Protonated IL [C3MIM$^+$][I^-]. Further increase of temperature shows temperature in dependence of dc-conductivity.

This reflected the thermally activated ion hopping over an energy barrier E_A up to the some characteristic temperature, after which there is no effect of heating in the activation of the ion hopping process. The coincidence at lower temperature is somewhat anomalous since the coupling between conductivity viscosity and glass transition temperature as well is expected. The two ionic liquids under investigations are completely different in both viscosity (C2- methylated [C3DMIM$^+$][I^-] is solid at room temperature) and glass transition. Enhancement of conductivity is also expected with reducing glass transition which is not the case here at least at relatively lower temperatures. The coupling between conductivity and viscosity was found to be varying in many recent studies of different ionic liquids [52–54].

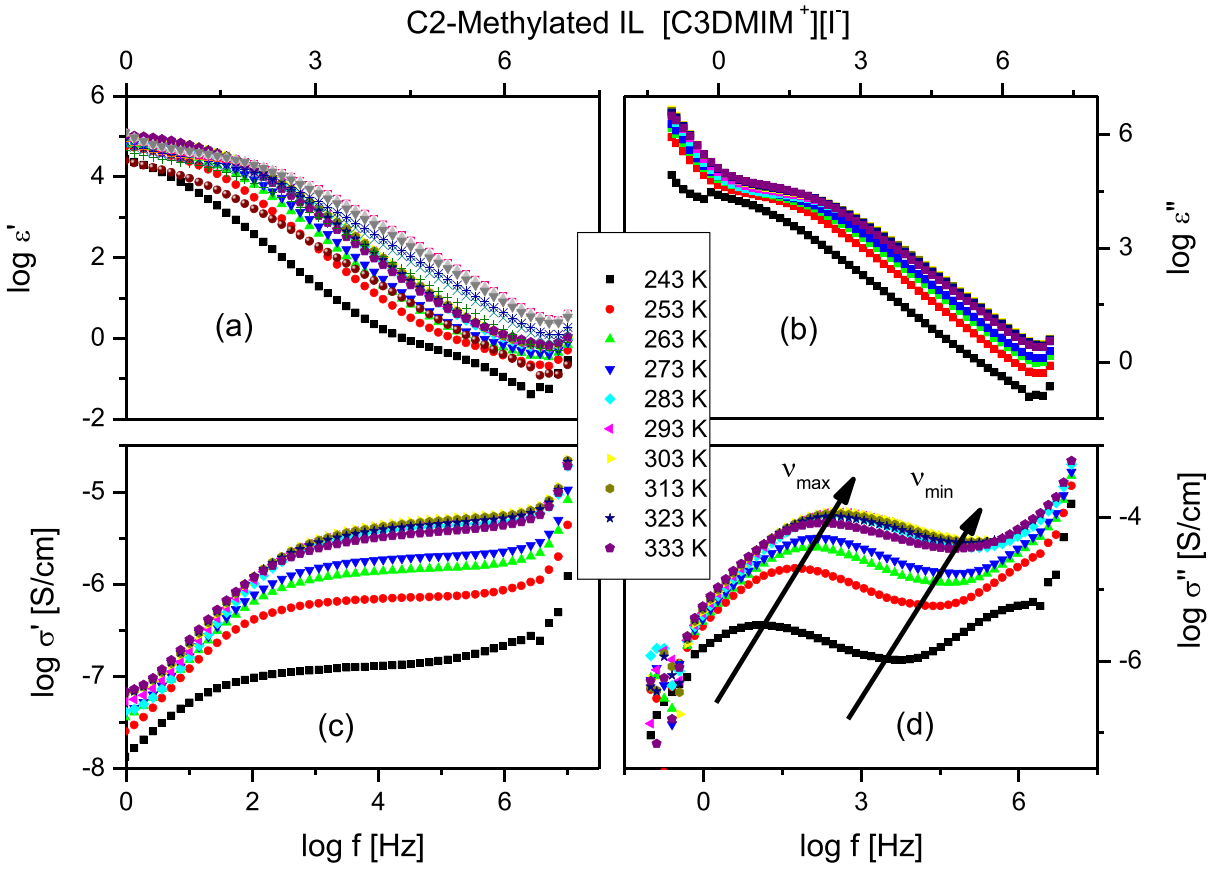

Fig. 5. Complex dielectric permittivity and conductivity as function of frequency at different temperatures for versus C2-Methylated [C_3DMIM $^+$][I^-].

The dissipation factor (usually called tan δ) D ($=\frac{\varepsilon)}{\varepsilon'}$) investigation may suppresses undesirable capacitance effects due to electrode contacts at least at temperatures under considerations and provides a clear peak of the dc conduction. D (usually called *tanδ*) is presented against frequency at different temperatures for both investigated ionic liquids as shown in Fig. 6. *Tanδ* spectra show a peak- its maximum position characterizes what is called the conductivity hopping time. The peak shifts towards higher frequency i.e. the dynamic became faster, with increasing temperature which is not the case at higher temperatures [55,56].

The dissipation factor (*tanδ*) as illustrated graphically against frequency can be used to define what called conductivity-relaxation time $\tau_{\sigma D}$. This relaxation time supposed to be equivalent to the hopping time and characterizes the ionic dynamics. The peak of *tanδ* as a function of frequency thought to ascribed the translational ionic motions and $\tau_{\sigma D}$ is determined from the frequency at the maximum peak position$f_{max}(= 1/(2\pi\tau_{\sigma D})$. We are convinced that the peak in *tanδ* spectra originated from relaxation of conductivity since it is accompanied by the frequency independent range of conductivity (characterizing the dc-conductivity) and not a peak in the ε'' (ν) spectra. In other words; this peak does not characterize any orientational dynamic at molecular scale or any terminal groups' dynamics but describes the translational motions of ionics.

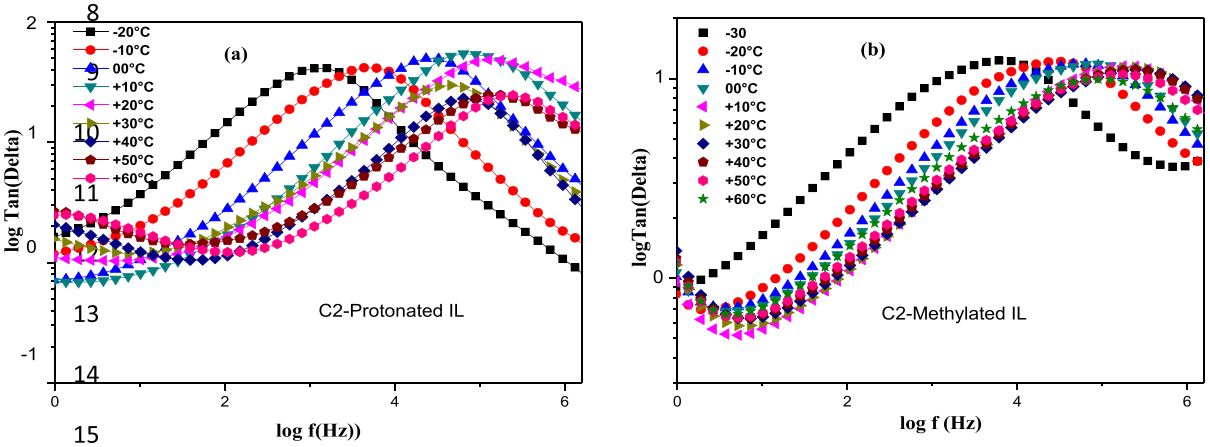

Fig. 6. Temperature dependence of loss tangent (*tanδ*) for C2-Protonated [C_3MIM^+][I^-] (a) versus C2-Methylated [C_3DMIM $^+$][I^-] (b).

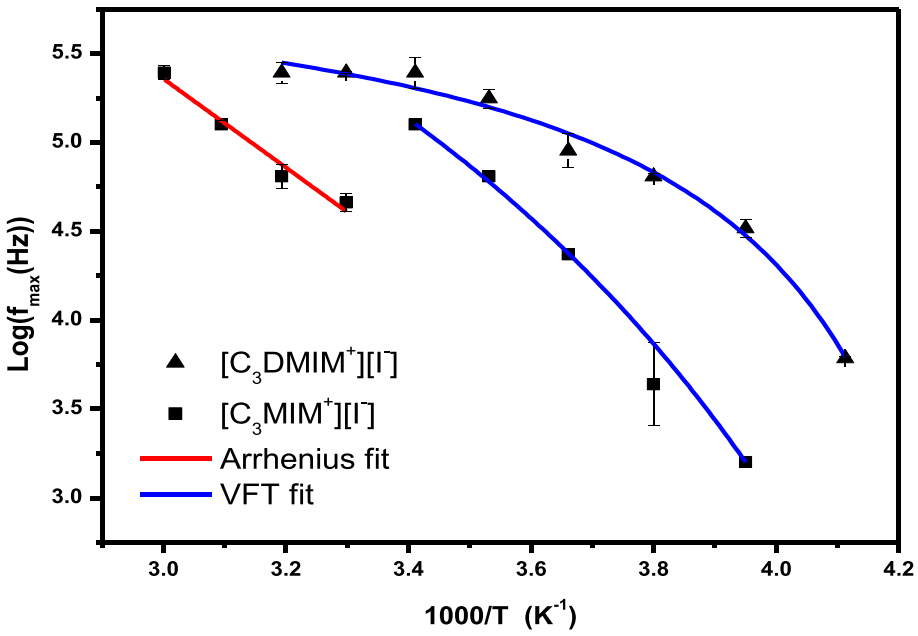

Fig. 7. Temperature dependence of the relaxation frequency peaks for the C2-Methylated IL [C_3DMIM $^+$][I^-] and the C2-Protonated IL [C_3MIM$^+$][I^-].

Table 2
Activation energies for the C2-Methylated IL [C_3DMIM$^+$][I^-] and the C2-Protonated IL [C_3MIM$^+$][I^-].

[C_3MIM$^+$][I^-]				[C_3DMIM$^+$][I^-]	
Arrhenius	R^2(corr.coef.)	VFT	R^2(corr.coef.)	VFT	R^2(corr.coef.)
0.215 eV	0.957	0.063 eV	0.998	0.010 eV	0.999

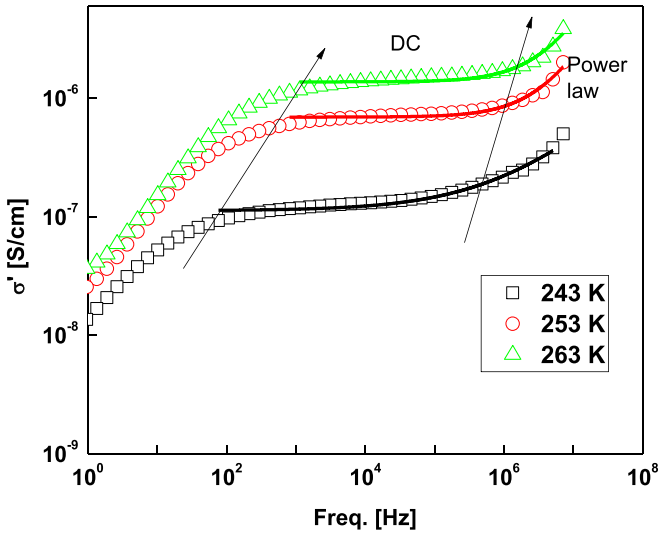

Fig. 8. Real part of complex conductivity function against frequency for C2- methylated [C3DMIM$^+$][I^-] at the indicated temperatures. Lines are fits of the Jonscher equation.

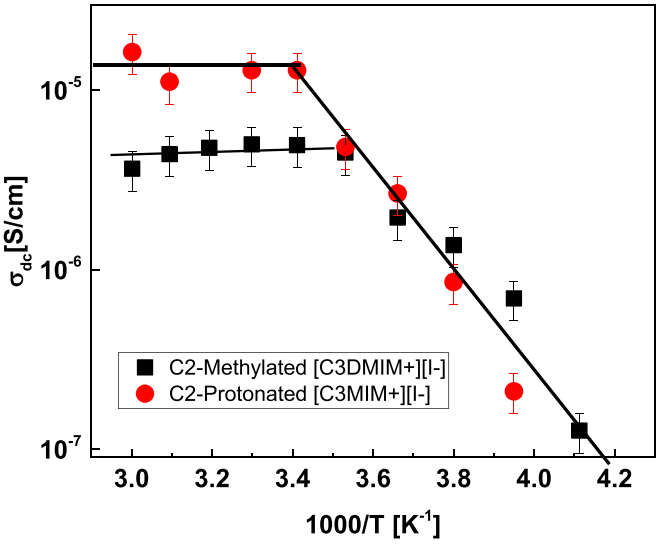

Fig. 9. DC-conductivity σ_{DC} versus 1000/T for the two ionic liquids under investigations as indicated. The solid lines are linear regression using all data points.

4. Conclusion

Synthesis and characterization of C2-Methylated [C_3DMIM$^+$][I^-] versus C2-Protonated ILs has been reported. The structure of both ILs was identified by using ^{1}H, ^{13}C NMR. The dielectric measurements in the temperature range of −30 °C to 60 °C have been performed in the frequency range from (10^{-2} to 10^7 Hz). Based on the experimental results and above discussion, following conclusions were obtained. The thermal behavior confirmed that the methylated [C_3DMIM$^+$][I^-] IL is thermally more stable than the protonated one [C_3MIM$^+$][I^-]. The dielectric data show two different behaviors: The temperature dependence of relaxation times of the protonated [C_3MIM$^+$][I^-] described by the Vogel-Fulcher-Tamman (VFT) law in the temperature range of −20–20 °C and by the Arrhenius law in the temperature range of 20–60 °C, while, only VFT-like temperature dependence in the entire investigated temperature range from −30 °C to 60 °C for the methylated IL [C_3DMIM $^+$][I^-]. Also, the differences in the apparent activation energies in relaxation processes may be related to the decoupling phenomenon between ion migration and structural relaxation times. On the other hand, analysis of the conductivity spectra shows that the charge

carriers transport accompanied by the electrode polarization are the main dynamics processes could be determined and they screened out any contribution of other dynamic processes at the molecular or sub-molecular scales.

Declaration of Competing Interest

None.

Acknowledgement

HB gratefully acknowledges the financial support by The Ministry of Higher Education and Scientific Research (MESRS) of Algeria in PRFU project code: B00L01UN200120180002. Also, Authors affiliated to Synthesis and Catalysis Laboratory thank the ATRST-DGRSDT for financial support and Professor Freidrich KREMER (University of Leipzig) for his valuable advice on this article.

References

[1] K. Nakajima, M. Lísal, K. Kimura, Surfaces of ionic liquids, Surf. Interf. Sci. Liquid Biol. Interf. 7 (2020) 351–389.
[2] M. Kar, O. Tutusaus, D.R. MacFarlane, R. Mohtadi, Novel and versatile room temperature ionic liquids for energy storage, Energy Environ. Sci. 12 (2) (2019) 566–571.
[3] R. Sulaiman, M.K. Hadj-Kali, S.W. Hasan, S. Mulyono, I.M. AlNashef, Investigating the solubility of chlorophenols in hydrophobic ionic liquids, J. Chem. Thermodyn. 135 (2019) 97–106.
[4] A.R. Jesus, M.R. Soromenho, L.R. Raposo, J.M. Esperança, P.V. Baptista, A.R. Fernandes, P.M. Reis, Enhancement of water solubility of poorly water-soluble drugs by new biocompatible N-acetyl amino acid N-alkyl cholinium-based ionic liquids, Eur. J. Pharm. Biopharm. 137 (2019) 227–232.
[5] P. Yoganantharajah, D.J. Eyckens, J.L. Pedrina, L.C. Henderson, Y. Gibert, A study on acute toxicity and solvent capacity of solvate ionic liquids in vivo using a zebrafish model (Daniorerio), New J. Chem. 40 (8) (2016) 6599–6603.
[6] D.R. MacFarlane, N. Tachikawa, M. Forsyth, J.M. Pringle, P.C. Howlett, G.D. Elliott, ... C.A. Angell, Energy applications of ionic liquids, Energy & Environmental Science 7 (1) (2014) 232–250.
[7] G.B. Appetecchi, G.T. Kim, M. Montanino, M. Carewska, R. Marcilla, D. Mecerreyes, I. De Meatza, Ternary polymer electrolytes containing pyrrolidinium-based polymeric ionic liquids for lithium batteries, J. Power Sources 195 (11) (2010) 3668–3675.
[8] H. Tokuda, K. Hayamizu, K. Ishii, M.A.B.H. Susan, M. Watanabe, Physicochemical properties and structures of room temperature ionic liquids. 2. Variation of alkyl chain length in imidazoliumcation, J. Phys. Chem. B 109 (13) (2005) 6103–6110.
[9] M.P. Singh, R.K. Singh, S. Chandra, Ionic liquids confined in porous matrices: physicochemical properties and applications, Prog. Mater. Sci. 64 (2014) 73–120.
[10] F. Endres, A. Abbott, in: D. MacFarlane (Ed.), Electrodeposition from Ionic Liquids, John Wiley & Sons, 2017.
[11] M.V. Fedorov, A.A. Kornyshev, Ionic liquids at electrified interfaces, Chem. Rev. 114 (5) (2014) 2978–3036.
[12] Y. Cao, T. Mu, Comprehensive investigation on the thermal stability of 66 ionic liquids by thermogravimetric analysis, Ind. Eng. Chem. Res. 53 (20) (2014) 8651–8664.
[13] C. Maton, N. De Vos, C.V. Stevens, Ionic liquid thermal stabilities: decomposition mechanisms and analysis tools, Chem. Soc. Rev. 42 (13) (2013) 5963–5977.
[14] M.T. Clough, K. Geyer, P.A. Hunt, J. Mertes, T. Welton, Thermal decomposition of carboxylate ionic liquids: trends and mechanisms, Phys. Chem. Chem. Phys. 15 (47) (2013) 20480–20495.
[15] P. Navarro, M. Larriba, E. Rojo, J. García, F. Rodríguez, Thermal properties of cyano-based ionic liquids, J. Chem. Eng. Data 58 (8) (2013) 2187–2193.
[16] B.G. Soares, K. Pontes, J.A. Marins, L.F. Calheiros, S. Livi, G.M. Barra, Poly (vinylidene fluoride-co-hexafluoropropylene)/polyaniline blends assisted by phosphonium–based ionic liquid: dielectric properties and β-phase formation, Eur. Polym. J. 73 (2015) 65–74.
[17] J.R. Sangoro, C. Iacob, A.L. Agapov, Y. Wang, S. Berdzinski, H. Rexhausen, ... F. Kremer, Decoupling of ionic conductivity from structural dynamics in polymerized ionic liquids, Soft Matter 10 (20) (2014) 3536–3540.
[18] J. Sangoro, T. Cosby, F. Kremer, Rotational and translational diffusion in ionic liquids, Dielectric Properties of Ionic Liquids, Springer International Publishing 2016, pp. 29–51.
[19] X.X. Zhang, C. Schröder, N.P. Ernsting, Communication: solvation and dielectric response in ionic liquids—conductivity extension of the continuum model, J. Chem. Phys. 138 (2013) 111102.
[20] P.J. Griffin, A.P. Holt, K. Tsunashima, J.R. Sangoro, F. Kremer, A.P. Sokolov, Ion transport and structural dynamics in homologous ammonium and phosphonium-based room temperature ionic liquids, J. Chem. Phys. 142 (8) (2015), 084501, .
[21] E.I. Izgorodina, R. Maganti, V. Armel, P.M. Dean, J.M. Pringle, K.R. Seddon, D.R. MacFarlane, Understanding the effect of the C2 proton in promoting low viscosities and high conductivities in imidazolium-based ionic liquids: part I. weakly coordinating anions, J. Phys. Chem. B 115 (49) (2011) 14688–14697.
[22] H. Luo, G.A. Baker, S. Dai, Isothermogravimetric determination of the enthalpies of vaporization of 1-alkyl-3-methylimidazolium ionic liquids, J. Phys. Chem. B 112 (33) (2008) 10077–10081.
[23] R. Ludwig, D. Paschek, Applying the inductive effect for synthesizing low-melting and low-viscosity Imidazolium-based ionic liquids, ChemPhysChem 10 (3) (2009) 516–519.
[24] Y. Zhang, E.J. Maginn, The effect of C2 substitution on melting point and liquid phase dynamics of imidazolium based-ionic liquids: insights from molecular dynamics simulations, Phys. Chem. Chem. Phys. 14 (35) (2012) 12157–12164.
[25] T. Endo, T. Kato, K. Nishikawa, Effects of methylation at the 2 position of the cation ring on phase behaviors and conformational structures of imidazolium-based ionic liquids, J. Phys. Chem. B 114 (28) (2010) 9201–9208.
[26] H. Weingärtner, The static dielectric permittivity of ionic liquids, J. Mol. Liq. 192 (2014) 185–190.
[27] M.M. Huang, Y. Jiang, P. Sasisanker, G.W. Driver, H. Weingärtner, Static relative dielectric permittivities of ionic liquids at 25 C, J. Chem. Eng. Data 56 (4) (2011) 1494–1499.
[28] T. Endo, M. Imanari, H. Seki, K. Nishikawa, Effects of methylation at position 2 of cation ring on rotational dynamics of imidazolium-based ionic liquids investigated by NMR spectroscopy:[C4mim] Br vs [C4C1mim] Br, J. Phys. Chem. A 115 (14) (2011) 2999–3005.
[29] B. Haddad, D. Mokhtar, M. Goussem, E.H. Belarbi, D. Villemin, S. Bresson, ... J. Kiefer, Influence of methyl and propyl groups on the vibrational spectra of two imidazolium ionic liquids and their non-ionic precursors, Journal of Molecular Structure 1134 (2017) 582–590.
[30] M.A. Moussa, A.M. Ghoneim, M.H. Abdel Rehim, S.A. Khairy, M.A. Soliman, G.M. Turky, Relaxation dynamic and electrical mobility for poly (methyl methacrylate)-polyaniline composites, J. Appl. Polym. Sci. 134 (42) (2017) 45415.
[31] F. Kremer, A. Schönhals, in: F. Kremer, A. Schönhals (Eds.), Broadband Dielectric Spectroscopy, Springer, Berlin, Germany, 2002.
[32] S.H. El-Sabbagh, N.M. Ahmed, G.M. Turky, M.M. Selim, Rubber nanocomposites with new core-shell metal oxides as nanofillers, Progress in Rubber Nanocomposites, Woodhead Publishing 2017, pp. 249–283.
[33] A. Kyritsis, K. Raftopoulos, M.A. Rehim, S.S. Shabaan, A. Ghoneim, G. Turky, Structure and molecular dynamics of hyperbranched polymeric systems with urethane and urea linkages, Polymer 50 (16) (2009) 4039–4047.
[34] H.L. Ngo, K. LeCompte, L. Hargens, A.B. McEwen, Thermal properties of imidazolium ionic liquids, ThermochimicaActa 357 (2000) 97–102.
[35] W.H. Awad, J.W. Gilman, M. Nyden, R.H. Harris, T.E. Sutto, J. Callahan, ... D.M. Fox, Thermal degradation studies of alkyl-imidazolium salts and their application in nanocomposites, ThermochimicaActa 409 (1) (2004) 3–11.
[36] C. Maton, N. De Vos, C.V. Stevens, Ionic liquid thermal stabilities: decomposition mechanisms and analysis tools, Chem. Soc. Rev. 42 (13) (2013) 5963–5977.
[37] J.R. Sangoro, C. Iacob, S. Naumov, R. Valiullin, H. Rexhausen, J. Hunger, ... F. Kremer, Diffusion in ionic liquids: the interplay between molecular structure and dynamics, Soft Matter 7 (5) (2011) 1678–1681.
[38] C. Krause, J.R. Sangoro, C. Iacob, F. Kremer, Charge transport and dipolar relaxations in imidazolium-based ionic liquids, J. Phys. Chem. B 114 (1) (2009) 382–386.
[39] C. Iacob, J.R. Sangoro, A. Serghei, S. Naumov, Y. Korth, J. Kärger, ... F. Kremer, Charge transport and glassy dynamics in imidazole-based liquids, The Journal of chemical physics 129 (23) (2008) 234511.
[40] S. Zahn, G. Bruns, J. Thar, B. Kirchner, What keeps ionic liquids in flow? Phys. Chem. Chem. Phys. 10 (46) (2008) 6921–6924.
[41] S.B. Lehmann, M. Roatsch, M. Schöppke, B. Kirchner, On the physical origin of the cation–anion intermediate bond in ionic liquids part I. placing a (weak) hydrogen bond between two charges, Phys. Chem. Chem. Phys. 12 (27) (2010) 7473–7486.
[42] E.I. Izgorodina, R. Maganti, V. Armel, P.M. Dean, J.M. Pringle, K.R. Seddon, D.R. MacFarlane, Understanding the effect of the C2 proton in promoting low viscosities and high conductivities in imidazolium-based ionic liquids: part I. weakly coordinating anions, J. Phys. Chem. B 115 (49) (2011) 14688–14697.
[43] K. Nakamura, T. Shikata, Systematic dielectric and NMR study of the ionic liquid 1-Alkyl-3-methyl Imidazolium, ChemPhysChem 11 (1) (2010) 285–294.
[44] A.S. Rodrigues, M.A. Rocha, H.F. Almeida, C.M. Neves, J.A. Lopes-da-Silva, M.G. Freire, ... L.M. Santos, Effect of the Methylation and N–H Acidic Group on the Physicochemical Properties of imidazolium-Based Ionic Liquids, The Journal of Physical Chemistry B 119 (28) (2015) 8781–8792.
[45] M.J. Monteiro, F.F. Bazito, L.J. Siqueira, M.C. Ribeiro, R.M. Torresi, Transport coefficients, Raman spectroscopy, and computer simulation of lithium salt solutions in an ionic liquid, J. Phys. Chem. B 112 (7) (2008) 2102–2109.
[46] K. Nakamura, K. Fukao, Dielectric relaxation behavior of polymerized ionic liquids with various charge densities, Polymer 54 (13) (2013) 3306–3313.
[47] Z. Wojnarowska, J. Knapik, M. Díaz, A. Ortiz, I. Ortiz, M. Paluch, Conductivity mechanism in polymerized imidazolium-based protic ionic liquid [HSO3–BVIm][OTf]: dielectric relaxation studies, Macromolecules 47 (12) (2014) 4056–4065.
[48] C. Liao, N. Shao, K.S. Han, X.G. Sun, D.E. Jiang, E.W. Hagaman, S. Dai, Physicochemical properties of imidazolium-derived ionic liquids with different C-2 substitutions, Phys. Chem. Chem. Phys. 13 (48) (2011) 21503–21510.
[49] J.L. Barton, Dielectric relaxation of some ternary alkali-alkaline earth-silicate glasses, Verres Refract 20 (5) (1966) 328–335.
[50] T. Nakajima, 1971 Annual Report, Conference on Electric Insulation and Dielectric Phenomena, National Academy of Sciences, Washington DC, 1972.
[51] H. Namikawa, Characterization of the diffusion process in oxide glasses based on the correlation between electric conduction and dielectric relaxation, J. Non-Cryst. Solids 18 (2) (1975) 173–195.

[52] N. Ito, R. Richert, Solvation dynamics and electric field relaxation in an imidazolium-PF6 ionic liquid: from room temperature to the glass transition, J. Phys. Chem. B 111 (18) (2007) 5016–5022.
[53] P.J. Griffin, A.L. Agapov, A.P. Sokolov, Translation-rotation decoupling and nonexponentiality in room temperature ionic liquids, Phys. Rev. E 86 (2) (2012), 021508, .
[54] W. Xu, E.I. Cooper, C.A. Angell, Ionic liquids: ion mobilities, glass temperatures, and fragilities, J. Phys. Chem. B 107 (25) (2003) 6170–6178.
[55] Z. Wojnarowska, M. Paluch, Recent progress on dielectric properties of protic ionic liquids, J. Phys. Condens. Matter 27 (7) (2015), 073202, .
[56] K. Ueno, Z. Zhao, M. Watanabe, C.A. Angell, Protic ionic liquids based on decahydroisoquinoline: lost superfragility and ionicity-fragility correlation, J. Phys. Chem. B 116 (1) (2012) 63–70.